Impact of Vertical Wind Shear on Tropical Cyclone Rainfall

While tropical cyclone rainfall has a large axisymmetric component, previous observational (Lonfat et al. 2007; Chen et al. 2006; Cecil 2007; Ueno 2007) and theoretical (Jones 1995; DeMaria 1996; Frank and Ritchie 1999, 2001; Rogers et al. 2003; Ueno 2008) studies have shown that environmental vertical wind shear leads to an asymmetric component of the vertical motion and precipitation fields. Composites consistently depict a precipitation enhancement downshear and also cyclonically downwind from the downshear direction. For consistence with much of the literature and with Northern Hemisphere observations, this is subsequently referred to as "Downshear-Left". Stronger shear magnitudes are associated with greater amplitude precipitation asymmetries. Recent work has reinforced the prior findings, and explored details of the response of the precipitation and kinematic fields to environmental vertical wind shear. Much of this research has focused on tropical cyclones away from land, to limit the influence of other processes that might distort the signal related to vertical wind shear. Recent evidence (Yu et al. 2014) does suggest vertical wind shear can also play a major role in precipitation asymmetries during and after landfall.

Many observational studies use the 200-850 hPa wind vector difference averaged over several hundred kilometers to characterize the vertical wind shear. This is in part due to the availability of a 200-850 hPa shear value from the Statistical Hurricane Intensity Prediction Scheme (SHIPS; DeMaria et al. 2005). Wingo and Cecil (2010) showed that shear-relative rainfall composites from ~20,000 passive microwave satellite snapshots of >1000 tropical cyclones are generally similar (favoring the Downshear-Left region) whether considering deep-level (200-850 hPa), mid-level (500-850 hPa), or low-level (700-925 hPa) shear. They noted that these shear directions are usually similar to each other, and that the deep-level shear seems most important when considering the small subset of cases where these shear vectors are out of phase with each other. Wingo and Cecil (2010) also found a greater amplitude asymmetry in the rainfall composites for westerly shear than for easterly shear, but the Downshear-Left direction was favored regardless of shear direction. Similarly, the Downshear-Left direction is favored regardless of the storm motion direction, but the amplitude of the asymmetry varies. Wingo and Cecil (2010) considered cases with at least 5 m s^{-1} for both the shear magnitude and the storm motion. The asymmetry was greatest for cases with shear toward the right of the storm motion vector, such that the Downshear-Left and Front-Right quadrants coincide. Shear oriented toward the left of storm motion has the least asymmetry, and not coincidentally has a disproportionate share of major hurricanes in the sample. The magnitude of the shear-induced precipitation asymmetry decreases with increasing tropical cyclone intensity, possibly due to azimuthal advection of hydrometeors by the stronger winds. The shear-induced composited rainfall asymmetry is primarily a result of asymmetries in the heavy rain locations – rainfall occurrence (i.e., areal coverage at a given time) does not vary by quadrant as much as the rain rate magnitude does.

Yu et al. (2014) examined precipitation asymmetries in tropical cyclones making landfall in China and Taiwan, specifically considering different regions from south to north. They found that the Downshear and Downshear-Left precipitation enhancement dominates before, during, and after landfall in all regions (Figure 1). Landfalls in the southern provinces and Taiwan are dominated by east-northeasterly shear, and composited precipitation asymmetries favor the southwest and southern parts of the storms. The northernmost province studied by Yu et al. (2014), Zhejiang, more often has a westerly component of shear, and precipitation is enhanced in the

eastern (downshear) quadrants. Landfalls in this province are more likely to interact with the mid-latitude westerlies.

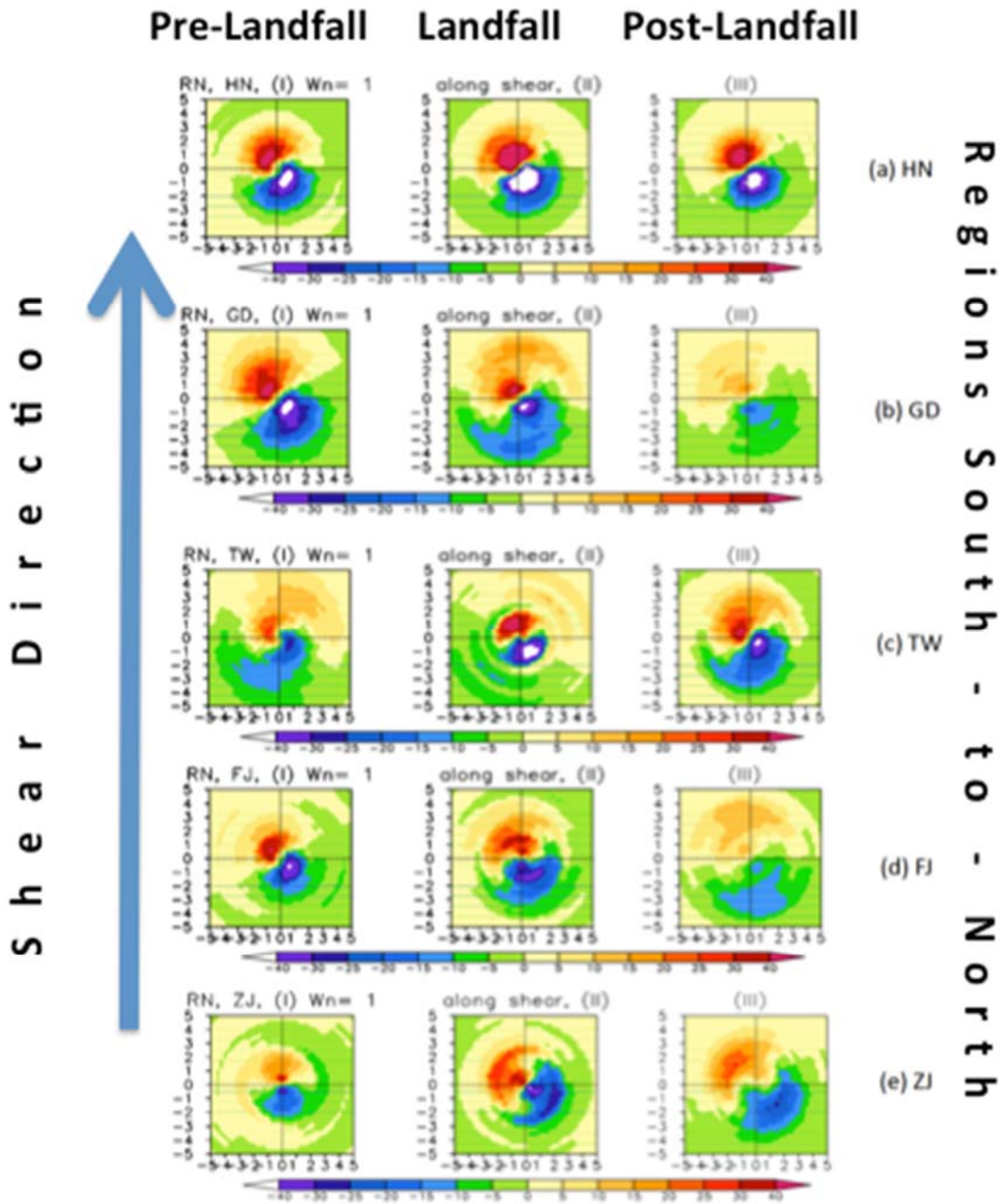

Figure 1. Shear-relative rainfall asymmetry before (left), during (middle), and after (right) landfall for regions of China and Taiwan. Regions progress from south at the top to north at the bottom of figure. Rainfall is maximized Downshear-Left in almost all composites. From Yu et al. (2014).

Much of the earlier theoretical research on shear-induced asymmetries has emphasized a tilted vortex in response to the vertical wind shear. Reasor et al. (2013) recently confirmed that the vortex does tilt in a downshear-left direction in observational composites from airborne radar in 75 hurricane flights. Reasor et al.'s composites for the hurricane core region feature convective initiation in the downshear-right region, peak ascent just left of the downshear direction, peak low-level reflectivities throughout the downshear-left quadrant, and the deepest radar echoes also in the downshear-left quadrant. Sinking motion is prevalent in the upshear-left quadrant, although advection carries a substantial amount of precipitation into this quadrant. Radar echoes are suppressed in the upshear-right quadrant in Reasor et al.'s aircraft-based composites.

This description of the radar structure is confirmed by Hence and Houze's (2011) analyses of hurricane eyewalls from the TRMM satellite's Precipitation Radar. Vertical reflectivity profiles from TRMM suggest convective development in the downshear-right quadrant, with maximum precipitation cyclonically downwind in the downshear-left quadrant. Hence and Houze (2011) noted that this pattern is rotated one quadrant clockwise for the unusual cases where the storm motion is greater than the vertical wind shear, and in nearly the opposite direction. The normally suppressed upshear-right quadrant features new convective development in those cases, with precipitation maximized downshear-right. Hence and Houze (2012) note that hurricane outer eyewalls show much less shear-induced asymmetry in the TRMM radar data. Concentric eyewall cases do have the previously described structure for the inner eyewall, but increasing shear only slightly favors the left-of-shear direction for strong convection in the outer eyewall.

DeHart et al. (2014) analyzed a subset of the airborne radar cases used by Reasor et al. (2013), with emphasis on the kinematic fields in the hurricane eyewall. Frequency distributions of vertical velocity (Figure 2) clearly show the shear-induced asymmetry, with more updrafts and fewer downdrafts in the downshear-right quadrant, relative to a frequency distribution for the entire eyewall. Cyclonically downwind in the downshear-left quadrant, there is a preference for *stronger* updrafts, particularly aloft. Downdrafts are favored and updrafts suppressed in the upshear quadrants, other than some weak upper-level updrafts in the upshear-right quadrant. Figure 3 applies the same analysis techniques to radar reflectivity. The combination of strong updrafts in the downshear-left quadrant and advection of precipitation that was generated in the downshear-right updrafts yields positive reflectivity anomalies in the downshear-left quadrant. The upshear-right is most suppressed, in terms of radar reflectivity. The schematic from DeHart et al. (2014) in Figure 4 here is consistent with the findings from many of the recent studies of shear-induced asymmetries: updrafts initiate in the downshear-right region and are maximized in the downshear-left. The upshear-left region has more downdrafts, and upshear-right has weaker vertical motion in general. These vertical motions coupled with horizontal advection of hydrometeors puts the greatest precipitation in the downshear-left, with the least upshear-right.

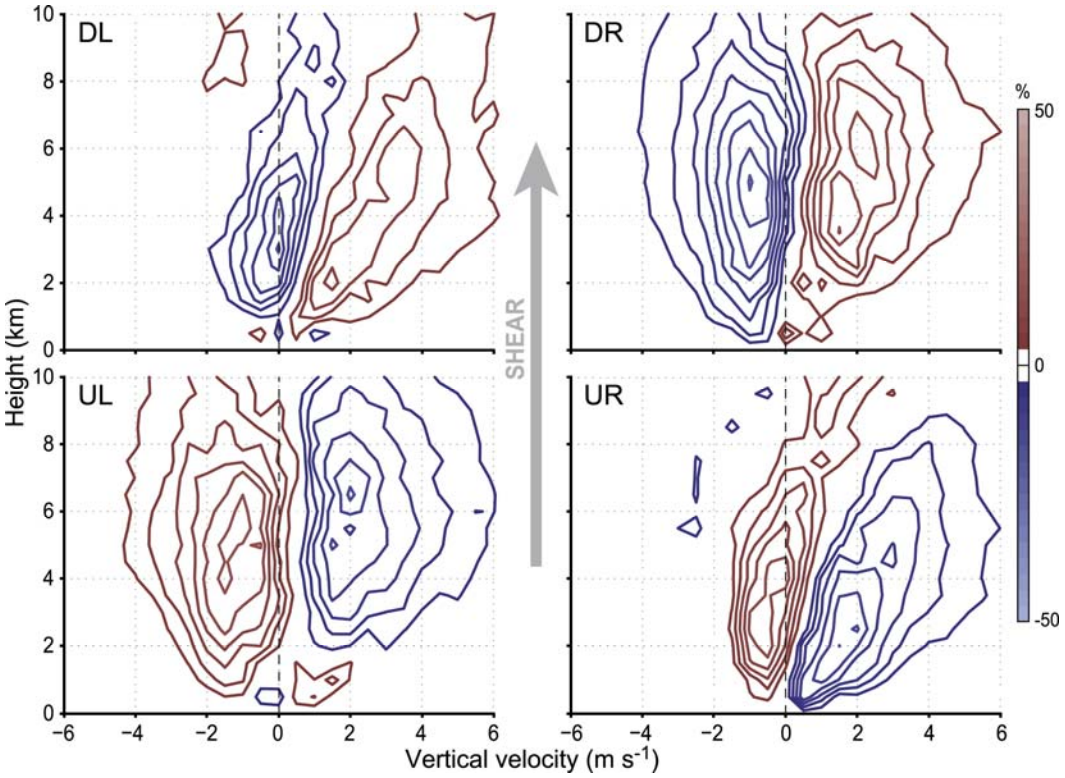

Figure 2. Anomaly Contoured Frequency by Altitude Display (CFAD) of eyewall vertical velocity for each shear-relative quadrant, relative to a CFAD for the eyewall in general. Contours represent the frequency anomaly, contoured every 5%, where red contours are positive anomalies and blue contours are negative anomalies. From DeHart et al. (2014)

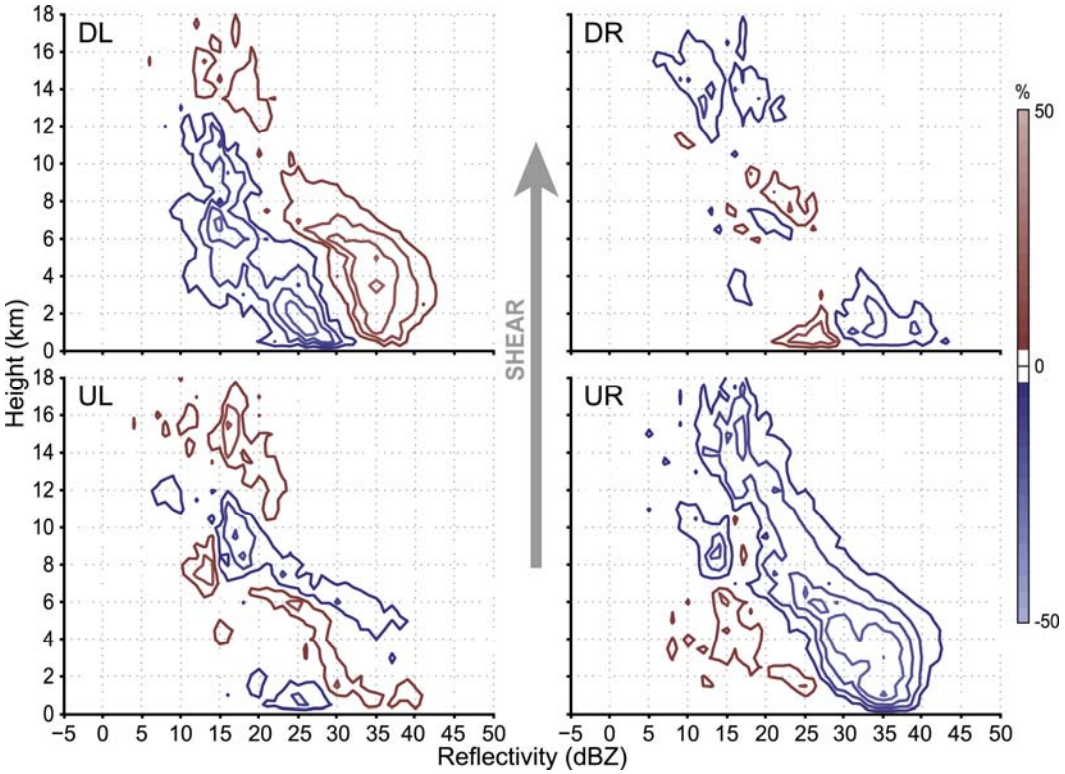

Figure 3. As in Figure 2, but for radar reflectivity. From DeHart et al. (2014).

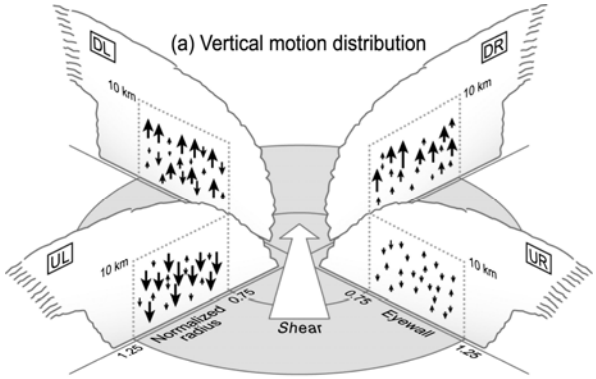

Figure 4. Schematic of the eyewall vertical motion distribution in each shear-relative quadrant. The environmental shear vector points toward the top of the figure.

References

Cecil, D.J., 2007: Satellite-derived rain rates in vertically sheared tropical cyclones. *Geophys. Res., Lett.*, **34**, L02811, doi:10.1029/2006GL027942.

Chen, S.S., J.A. Knaff, and F.D. Marks Jr., 2006: Effects of vertical wind shear and storm motion on tropical cyclone rainfall asymmetries deduced from TRMM. *Mon. Wea. Rev.*, **134**, 3190-3208.

DeHart, J.C., R.A. Houze, Jr., and R.F. Rogers, 2014: Quadrant distribution of tropical cyclone inner-core kinematics in relation to environmental shear. *J. Atmos. Sci.*, **71**, 2713-2732.

DeMaria, M. 1996: The effect of vertical shear on tropical cyclone intensity change. *J. Atmos. Sci.*, **53**, 2076-2088.

DeMaria, M., M. Mainelli, L.K. Shay, J.A. Knaff, and J. Kaplan, 2005: Further Improvements to the Statistical Hurricane Intensity Prediction Scheme (SHIPS). *Wea Forecasting*, **20**, 531-543.

Frank, W.M. and E.A. Ritchie, 1999: Effects of environmental flow upon tropical cyclone structure. *Mon. Wea. Rev*., **127**, 2044-2061.

---, and ---, 2001: Effects of vertical wind shear on the intensity and structure of numerically simulated hurricanes. *Mon. Wea. Rev*., **129**, 2249-2269.

Hence, D.A. and R.A. Houze Jr., 2011: Vertical structure of hurricane eyewalls as seen by TRMM Precipitation Radar. *J. Atmos. Sci*., **68**, 1637-1652.

---, and ---, 2012: Vertical structure of tropical cyclones with concentric eyewalls as seen by the TRMM Precipitation Radar. *J. Atmos. Sci*., **69**, 1021-1036.

Jones, S.C., 1995: The evolution of vortices in vertical shear: I: Initially barotropic vortices. *Quart. J. Roy. Meteor. Soc*., **121**, 821-851.

Lonfat, M., R. Rogers, T. Marchok, and F.D. Marks Jr., 2007: A parametric model for predicting hurricane rainfall. *Mon. Wea. Rev*., **135**, 3086-3097.

Reasor, P.D., R. Rogers, and S. Lorsolo, 2013: Environmental flow impacts on tropical cyclone structure diagnosed from airborne Doppler radar composites. *Mon. Wea. Rev*., **141**, 2949-2969.

Rogers, R., S. Chen, J. Tenerelli, and H. Willoughby, 2003: A numerical study of the impact of vertical shear on the distribution of rainfall in Hurricane Bonnie (1998). *Mon. Wea. Rev*., **131**, 1577-1599.

Ueno, M., 2007: Observational analysis and numerical evaluation of the effects of vertical wind shear on the rainfall asymmetry in the typhoon inner-core region. *J. Meteor. Soc. Japan*, **85**, 115-136.

---, 2008: Effects of vertical wind shear on the inner-core asymmetries and vertical tilt of a simulated tropical cyclone. *J. Meteor. Soc. Japan*, **86**, 531-555.

Wingo, M.T. and D.J. Cecil, 2010: Effects of vertical wind shear on tropical cyclone precipitation. *Mon. Wea. Rev*., **138**, 645-662.

Yu, Z., Y. Wang, and H. Xu, 2014: Observed rainfall asymmetry in tropical cyclones making landfall over China. *J. Appl. Meteor. Clim., in press*, http://dx.doi.org/10.1175/JAMC-D-13-0359.1.